Escape statistics for parameter sweeps through bifurcations

Nicholas J. Miller[1,2] and Steven W. Shaw[1]
[1]*Department of Mechanical Engineering, Michigan State University, East Lansing, Michigan 48824, USA*
[2]*Department of Physics and Astronomy, Michigan State University, East Lansing, Michigan 48824, USA*
(Received 11 October 2011; revised manuscript received 14 March 2012; published 4 April 2012)

We consider the dynamics of systems undergoing parameter sweeps through bifurcation points in the presence of noise. Of interest here are local codimension-one bifurcations that result in large excursions away from an operating point that is transitioning from stable to unstable during the sweep, since information about these "escape events" can be used for system identification, sensing, and other applications. The analysis is based on stochastic normal forms for the dynamic saddle-node and subcritical pitchfork bifurcations with a time-varying bifurcation parameter and additive noise. The results include formulation and numerical solution for the distribution of escape events in the general case and analytical approximations for delayed bifurcations for which escape occurs well beyond the corresponding quasistatic bifurcation points. These bifurcations result in amplitude jumps encountered during parameter sweeps and are particularly relevant to nano- and microelectromechanical systems, for which noise can play a significant role.

DOI: 10.1103/PhysRevE.85.046202 PACS number(s): 05.45.−a, 05.10.Gg, 05.40.Ca

I. INTRODUCTION

The problem of noise-activated escape out of a slowly changing potential or quasipotential well has a long history arising in a number of different fields. For example, in the 1970's the statistics of escape events from the zero voltage state in Josephson-junction circuits were examined to identify the junction parameter or critical current [1–3]. In this context, the escape events from the zero voltage to the running states provided a visible handle on systems that were otherwise difficult to measure or interrogate. In the late 1980's the related problem of delayed bifurcation received a great deal of attention in the study of laser turn-on dynamics [4–10]. Laser turn-on is described by a Hopf bifurcation or, in the rotating frame, a supercritical pitchfork bifurcation. Other examples of noisy swept systems near bifurcation points include nanomagnetics [11,12], in which escape dynamics lead to the confirmation of the Néel-Brown model; neuron dynamics [13], in which activated escape describes neuron firing; and tribology [14–16], in which microscopic stick-slip, or escape, events give rise to macroscopic friction. Additional relevant investigations include escape induced by Poisson noise [17], noise-induced bistability [18,19], and noise-induced chaos [20–23].

More recently, the problem of escape statistics has found relevance in applications in the Josephson bifurcation amplifier and its use for qubit readout [24–27], climate tipping [28], and bifurcation detection in nano- and microelectromechanical systems (NEMS and MEMS) [29,30]. The qubit detection application is particularly interesting, since the goal is to seek the optimal form for the parameter sweep trajectory that minimizes the overlap probability of escape for the two qubit states during a finite measurement time. In the climate tipping application, one is concerned with the estimation of the bifurcation point without allowing escape to occur, so that one can predict the possibility of an impending escape, which corresponds to sudden, drastic change in the climate. The NEMS and MEMS applications center around system identification and parametric sensing with NEMS and MEMS resonators. Many of these implementations mirror those of Josephson-junction circuits [26,27,31–37]. Accordingly, the sensing paradigms are very similar to those developed in the 1970's for measuring the Josephson-junction critical current. There is, however, one key difference. Many NEMS and MEMS devices experience effective noise forces that are much smaller than their Josephson counterparts, since they tend to be significantly more massive devices. Accordingly, a sweep toward a bifurcation in a NEMS and MEMS resonator may not result in activated escape before the bifurcation point is reached, but rather the device will experience a delayed bifurcation [29]. Therefore, it is necessary to understand the distribution of delayed bifurcation times in order to make effective use of parameter sweeping as a means of interrogating these systems. Moreover, quantifying the features which separate activated escape and delayed bifurcation will provide useful information to orient experimentalists working across all of these application areas.

Despite the interest in delayed bifurcations engendered by the study of laser turn-on dynamics, the authors have found only a few treatments of delayed saddle-node and subcritical pitchfork bifurcations. These bifurcations are common in NEMS and MEMS nonlinear resonators modeled by the Duffing and nonlinear Mathieu equations and so are of particular interest to us. In [38] scaling laws are developed that are directly applicable to the bifurcations considered here. However, in the present work we provide quantitative results about the distribution of escape events, as required for parameter identification and bifurcation-based sensing schemes.

For our discussion we use the term *bifurcation* to describe a change in the sign of the real part of an eigenvalue of an equilibrium point of the drift vector that results from a change of a parameter in a stochastic differential equation. The *bifurcation point* is understood as the condition in state and parameter space where the drift vector possesses an equilibrium point with an eigenvalue with zero real part. When discussing the dynamics of systems with a time-varying parameter, it is convenient to refer to the *bifurcation value* of

the parameter as that corresponding to the bifurcation point of the corresponding time-invariant system.

Here we derive a method for determining the statistics of the parameter values at which a system response will leave the vicinity of a bifurcating equilibrium point as a parameter is swept near the critical value in the presence of noise. This is carried out for the saddle-node and subcritical pitchfork bifurcations, both of which result in large excursions away from the bifurcating operating point. New approximate results for the escape event parameter distributions are obtained for the limit of small noise intensity relative to the parameter sweep rate (this limit is made precise in the subsequent formulation). These results, and the previously known adiabatic results [39,40], are compared with numerical solutions of the Fokker-Planck (FP) equation governing the distribution in the general case. The present analysis makes use of one-dimensional stochastic normal forms which describe the system dynamics local to a bifurcating fixed point in both phase space and parameter space. While our analysis is restricted to one-dimensional systems, higher dimensional systems with more complicated sweep trajectories can be reduced to this model when they exhibit separation of time scales and when the response escapes near the bifurcation point, so that the system dynamics are governed by a slow mode; that is, they occur on a slow one-dimensional manifold in the phase space [38,41,42].

As a result of escape near a bifurcation point, the system will exhibit a large transient and move into another region in phase space. In the case of activated escape, which occurs before the bifurcation point, the basin of attraction has a well-defined boundary, providing a clean definition of escape. In contrast, for delayed bifurcations there is ambiguity about the definition of escape, and thus also about the time at which it occurs, since the event occurs after the basin of attraction has disappeared. Some researchers have defined this escape problem in terms of a first passage time across a chosen threshold [6,7,9,10]. Others impose a threshold on the variance of the distribution [5,8], while another option is to consider the final crossing time of some threshold [13]. In the present study, the normal forms of interest are local models that exhibit escape to ∞ in finite time, which requires that the system trajectories become very steep enroute to ∞. Thus, we conclude that the time it takes to reach a large value of the coordinate of the local model of the slow mode is very close to the time taken to reach ∞, and we also assume that this large value is in the region where the one-dimensional normal form model breaks down. Accordingly, we say that an escape event occurs in the one-dimensional normal form when the coordinate along the slow manifold reaches $\pm\infty$, and we define the escape time to be the corresponding (finite) time. The attendant bifurcation value of the swept parameter is then known from its known time dependence. The statistics of these events is the focus of this work.

The use of local normal forms imposes some restrictions on the sweep rate and noise intensity. Specifically, in order for the local approximations made for the stochastic slow mode (center manifold) and normal form reductions to remain valid during the escape process, the noise intensity must be sufficiently small and the sweep rate sufficiently slow. As we show, the key parameter in a linear parameter sweep is the ratio of the sweep rate to the noise strength. We show that delayed bifurcation occurs without violating these assumptions. In addition, we also show that our solution is independent of initial conditions for a large class of initial conditions, owing to the fact that diffusive systems forget their initial conditions and settle into steady-state distributions [43], or quasi-steady-state distributions in the present case, since parameters are being varied. In this sense, the present formulation is quite general.

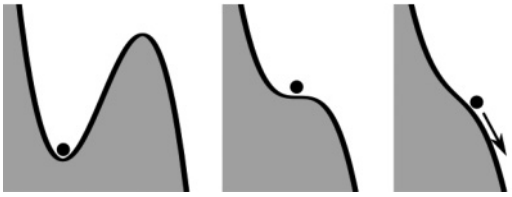

FIG. 1. Noisy dynamic saddle-node bifurcation.

It should be noted that the two problems considered here, namely, the saddle-node and subcritical pitchfork bifurcations, must be treated somewhat differently, since their zero-noise dynamics are qualitatively different. Specifically, escape is inevitable for the swept saddle node, whereas for the swept pitchfork a disturbance is required to induce escape from equilibrium, even when it is unstable, since the equilibrium persists past the bifurcation point. For both problems, the general result is formulated in terms of a FP equation. However, for the weak noise (delayed bifurcation) asymptotic results we use a variation of parameters approach to study the saddle-node bifurcation and matched asymptotic expansions for the subcritical pitchfork bifurcation. The analytically predicted distributions are compared with numerical solutions of the FP equation, demonstrating their accuracy and range of validity.

II. ESCAPE NEAR A SADDLE-NODE BIFURCATION

When sweeping a parameter near a saddle-node bifurcation, the dynamics along the slow manifold are described by a one-dimensional Langevin equation, i.e., the normal form, given by [38]:

$$\dot{x} = \mu(t) + x^2 + \epsilon\xi(t), \tag{1}$$

where $\mu(t)$ is the bifurcation parameter and $\xi(t)$ is zero-mean, delta-correlated white noise with autocorrelation $\langle\xi(t)\xi(t')\rangle = 2\delta(t-t')$. The dynamics of Eq. (1) are conveniently visualized by an overdamped particle moving in a time-varying potential, as illustrated in Fig. 1. Our goal is to determine the distribution of escape times T, that is, those for which $x \to \infty$ as $t \to T$. A numerical solution for this problem can be obtained by solving the FP equation associated with Eq. (1):

$$\frac{\partial\rho}{\partial t} = -\frac{\partial}{\partial x}[(\mu + x^2)\rho] + \epsilon^2\frac{\partial^2\rho}{\partial x^2}, \tag{2}$$

with appropriate initial and boundary conditions, the results of which are used to illustrate the connection between the fast and slow sweeping limits. We will later show that these limits are given by $\epsilon^2 \ll \dot{\mu}$ and $\epsilon^2 \gg \dot{\mu}$, respectively. For the slow sweeping (or, equivalently, the large noise) limit, consider that the system is initially near the local minimum of the potential

that exists for $\mu < 0$. If μ is increased slowly relative to the noise level, specifically, for $\epsilon^2 \gg \dot{\mu}$, one can approximate the rate of escape by the well-known adiabatic approximation due to Kramer [40,44]. For the saddle node, this rate is

$$W(t) = \frac{\sqrt{-\mu(t)}}{\pi} \exp\left\{ -\frac{4[-\mu(t)]^{3/2}}{3\epsilon^2} \right\}. \tag{3}$$

The probability to remain in the well diminishes according to the product of this rate and the probability to remain in the well. Accordingly, the probability density function (PDF) for escape at time T in the limit of adiabatic sweeping is given by [1,40]:

$$P(T) = W(T) \exp\left[-\int_{-t_0}^{T} W(t)dt \right]. \tag{4}$$

Of interest here is the case where the noise strength is small compared to the characteristic rate of change of the bifurcation parameter, that is, $0 \leqslant \epsilon^2 \ll \dot{\mu}$. In this case, the potential well will disappear before noise activated escape is likely to occur, and the system thus exhibits a delayed bifurcation, escaping to $x \to \infty$ at a finite time T, for which $\mu(T) > 0$. To approximate the distribution of escape times for Eq. (1) in this situation, we employ a direct perturbation method. To this end it is convenient to transform the equation using a variation of parameters approach, in which the $\epsilon = 0$ solution, x_0, plays the role of the homogeneous solution. The transformation $x_0 = -\dot{u}/u$ in Eq. (1) with $\epsilon = 0$ yields

$$\ddot{u} + \mu(t)u = 0, \tag{5}$$

which has linearly independent solutions u_1 and u_2, so that x_0 can be written as

$$x_0 = -\frac{\dot{u}_1 + c\dot{u}_2}{u_1 + cu_2}, \tag{6}$$

where c is a constant of integration. To account for the presence of noise, we let c vary in time. Utilizing expression (6) in Eq. (1) with $c(t)$ gives the equation for $c(t)$ as

$$\dot{c} = -\epsilon a(u_1 + cu_2)^2 \xi, \tag{7}$$

where $a^{-1} = u_1\dot{u}_2 - \dot{u}_1 u_2$ is the Wronskian. The variable c is a means of parametrizing the solutions of the noise-free problem, and the system diffuses among the noise-free trajectories according to Eq. (7).

The escape time T is given by the time at which x_0 becomes unbounded, which, according to Eq. (6), corresponds to $c(t)$ reaching the condition

$$c(t) = c_\infty(t) = -\frac{u_1(t)}{u_2(t)}, \qquad T \equiv t, \tag{8}$$

where $T \equiv t$ is meant to imply that T is defined as the time t at which this, $c = c_\infty$, condition is met. Here the first passage time problem reduces to a simple transformation of the stochastic variable $c(t)$ to the times T for which $c(T) = c_\infty(T)$, for some initial distribution of initial conditions. To determine the distribution of T, it is useful to consider the features of $c_\infty(t)$. The function $c_\infty(t)$ has branches, separated by vertical asymptotes at the zeros of $u_2(t)$, and $c(t)$ evolves between these branches. Figure 2 shows the first two branches of this boundary for a linear sweep trajectory. The two branches are

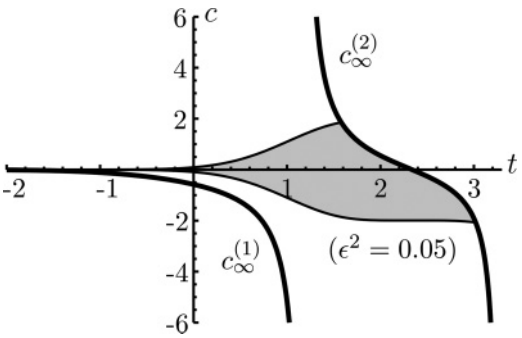

FIG. 2. c_∞ boundary for linear sweeping, $\mu(t) = \mu_0 + rt$, with $\mu_0 < 0$. The first two branches are shown along with the variance (shaded region) of c for $\epsilon^2 = 0.05$.

labeled $c_\infty^{(1)}$ and $c_\infty^{(2)}$. In addition, the shaded region shows the width, ± 3 standard deviations, of the distribution for $c(t)$, illustrating how escape to $x = \infty$ has become a first passage time problem across $c = c_\infty^{(2)}$. Also, note that since

$$\frac{dc_\infty}{dt} = \frac{1}{au_2^2} \tag{9}$$

does not change sign, $c_\infty(t)$ is monotonic between branches. In addition, by considering Eqs. (7) and (8), it is seen that $\dot{c} = 0$ when $c = c_\infty$. Thus, trajectories of $c(t)$ cross each branch of $c_\infty(t)$ at a single time. Consequently, in considering the first passage time of $c(t)$ across a particular branch of $c_\infty(t)$, we do not need to account for trajectories that cross $c_\infty(t)$ multiple times. We can therefore simplify our task by doing away with the adsorbing wall boundary condition commonly employed in first passage problems. This simplification brings an additional feature to our solution. Without an adsorbing wall boundary condition, a crossing corresponds to reinjection at $x = -\infty$. Hence, the system will again traverse the real line and subsequently reach $x = \infty$ again. This corresponds to a subsequent crossing of c_∞ occurring on the immediately subsequent branch only, and precisely at the times when the system becomes unbounded, that is, when $x \to \infty$. However, by identifying the branch corresponding to the first crossing, we may focus our solution on the escape time of interest.

The change of coordinates from $x(t)$ to $c(t)$ makes the problem amenable to direct perturbation analysis of Eq. (7). To develop a first-order asymptotic approximation of the escape current, we begin with the expansion

$$c = c_0 + \epsilon c_1 + \ldots. \tag{10}$$

Substitution of this into Eq. (7) and expansion in powers of ϵ yield

$$\dot{c}_0 = 0, \tag{11}$$

$$\dot{c}_1 = -a(u_1 + c_0 u_2)^2 \xi. \tag{12}$$

Note that the first-order perturbation removes the state-dependent diffusion, and thus Ito and Stratonovich calculus give the same result at this order. Solving Eqs. (11) and (12) gives a time-dependent Gaussian PDF for the noisy response

of c, as follows:

$$P_c(c,t) = \left[4\pi a^2\epsilon^2 \int_{t_0}^{t} (u_1 + c_0u_2)^4 dt'\right]^{-1/2} \times \exp\left[-\frac{(c-c_0)^2}{4a^2\epsilon^2 \int_{t_0}^{t}(u_1 + c_0u_2)^4 dt'}\right]. \quad (13)$$

Using this result, the PDF of escape times can be expressed as

$$P_\infty(T) = P_c(c_\infty, T)\left|\frac{dc_\infty(T)}{dT}\right|. \quad (14)$$

Combining Eqs. (9), (13), and (14), we arrive at an expression for the PDF of escape times:

$$P_\infty(T) = \left[4\pi a^4\epsilon^2 u_2^4(T) \int_{t_0}^{T} (u_1 + c_0u_2)^4 dt\right]^{-1/2} \times \exp\left\{-\frac{[u_1(T) + c_0u_2(T)]^2}{4a^2\epsilon^2 u_2^2(T) \int_{t_0}^{T}(u_1 + c_0u_2)^4 dt}\right\}. \quad (15)$$

Note that this result is quite general, since the form of the parameter sweep $\mu(t)$, which dictates $u_{1,2}(t)$, is not yet specified. The only constraint is that the perturbation remain valid, and thus ϵc_1 remains a small correction. An important example of $\mu(t)$ is considered next.

The simplest method for sweeping the bifurcation parameter is linear in time, that is, $\mu = \mu_0 + rt$, with $\mu_0 < 0$ and $r > 0$. The affine relationship between the bifurcation parameter and time allows one to identify the bifurcation parameter as a renormalized time variable. Thus, without loss of generality, we take $\mu = t$. With this form of sweeping, Eq. (5) becomes Airy's equation in backward time, that is, $\ddot{u} + tu = 0$, with independent solutions:

$$u_1(t) = A_i(-t), \quad (16)$$

$$u_2(t) = B_i(-t), \quad (17)$$

where A_i and B_i are the standard Airy functions, for which the standard parameter $a = -\pi$ [45]. In principle, u_1 and u_2 can be taken as linear combinations of A_i and B_i; however, the present choice is most convenient here. The first two branches of the c_∞ boundary, $c_\infty^{(1,2)}$, are shown in Fig. 2. In the weak noise case, only the second boundary can be crossed, since $c_\infty^{(1)}$ is bounded above by zero ($c_\infty^{(1)} < 0$) and monotonically decreases ($\dot{c}_\infty^{(1)} < 0$), while $c_0 > c_\infty^{(1)}$ must hold for initial conditions restricted to be near the minimum of the potential well. Thus, the only way to cross $c_\infty^{(1)}$ is for $c(t)$ to diffuse to $+\infty$ and be reinjected at $-\infty$, and this cannot happen under the weak noise assumption. Therefore, computing escape times, we consider only those trajectories that reach $c_\infty^{(2)}$. Note that $c_\infty^{(2)}$ spans the time interval between the first and second zeros of $B_i(-t)$, so that our approximation of the escape distribution times is necessarily limited to this time interval, which is given below. In principle, this time interval can be adjusted by taking a different linear combination of A_i and B_i for u_1 and u_2, since the time interval is specified by the zeros of u_2. However, as the perturbation solution requires small noise, the probability of escape outside this time interval is necessarily small.

Equation (15) captures the escape distribution with the system initially situated on the noise-free trajectory specified by c_0 at time t_0. Generally, the dependence on c_0 and t_0 becomes weak as $|t_0|$ becomes large since

$$c \sim e^{-\frac{2}{3}|t_0|^{3/2}}, \quad (18)$$

assuming the system begins the sweep near the bottom of the potential well. This weak dependence on this class of initial conditions is a property of the deterministic system and results from the annihilation of the fixed point after the bifurcation. While it is not captured in our perturbation, diffusion only increases this effect as the system settles into a quasi-steady-state distribution early in the sweep. Thus, when the sweep is started well before the bifurcation point, the initial conditions are forgotten.

With this understanding, the initial conditions for the linear sweep are taken to be $c_0 = 0$ and $t_0 = -\infty$. The resulting escape distribution then applies to all initial conditions where c_0 is near zero and $t_0 \ll -1$. The corresponding escape current is computed using Eqs. (15) and (17), resulting in

$$P_\infty(T) = \left[4\pi^5\epsilon^2 B_i^4(-T) \int_{-\infty}^{T} A_i^4(-t)dt\right]^{-1/2} \times \exp\left[\frac{-A_i^2(-T)}{4\pi^2\epsilon^2 B_i^2(-T) \int_{-\infty}^{T} A_i^4(-t)dt}\right], \quad (19)$$

with T restricted to the range between the first two zeros of $B_i(-t)$, $1.17 < t < 3.27$.

Equation (19) is a primary result for the saddle-node bifurcation with linear parameter sweep. We illustrate various features of this result in Fig. 3. Figure 3(a) shows the mean (black) and variance (gray) of the escape time distribution for a wide range of noise strengths, spanning adiabatic (Kramers) escape and delayed bifurcation. Solid lines are used to show the solution obtained by numerically solving the FP equation over a finite domain. The moments for the adiabatic approximation and the approximation developed here are shown as dashed lines over their respectively valid regions of the noise strength parameter. Two sample distributions are shown in Figs. 3(b) and 3(c). The distribution shown in Fig. 3(b) is for the adiabatic case, such that escape occurs before the bifurcation point, hence the negative values of escape times T. The distribution shown in Fig. 3(c) is for a weak noise (or relatively fast sweep rate), resulting in delayed bifurcation, and the distribution is restricted to the normalized time window $1.17 < T < 3.27$. Recall that here the escape times T are the same as the attendant bifurcation parameter values, μ_T.

Note that the variance is dramatically larger in the adiabatic case, $\epsilon^2 \gg 1$, when compared to the nonadiabatic case, $\epsilon^2 \ll 1$. This is the result of the different escape mechanisms in these two limiting cases. In the adiabatic case, escape is a rare event in which the noise overcomes a potential barrier. Thus, the probability of escape over a small time interval is small, but the sweep takes a long time, so escape is virtually inevitable. In this way, the escape events have a relatively wide distribution. In contrast, for the nonadiabatic case, escape is inevitable, since the potential well disappears, and the solution closely follows the deterministic trajectory that would result from an initial condition at the bottom of the potential well. The escape times are randomly distributed about this trajectory due to diffusion. These observations also indicate why the mean

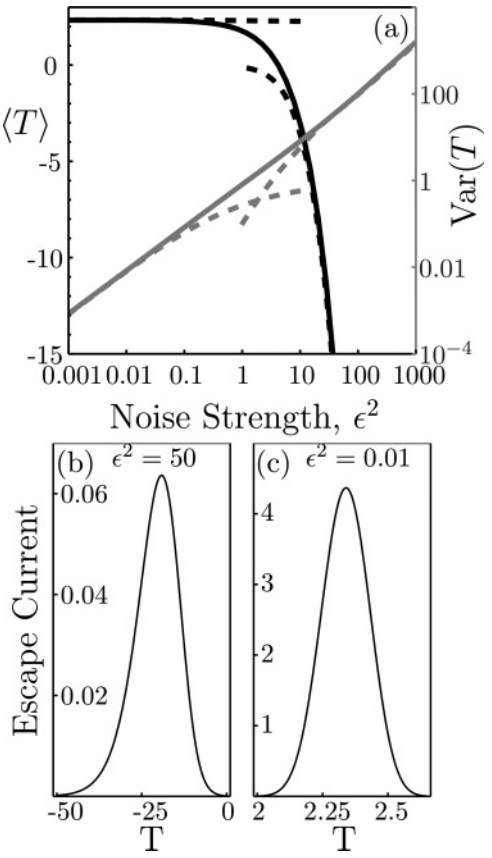

FIG. 3. (a) Mean (black) and variance (gray) of the escape current. Numeric solution (solid lines) and approximations (dashed lines) are shown. Two sample escape distributions are also shown, one for adiabatic escape (b) and one for delayed bifurcation (c).

escape time is insensitive to the noise strength for small noise intensity but highly sensitive to the noise strength for large noise intensity, as indicated in Fig. 3(a).

III. ESCAPE NEAR A SUBCRITICAL PITCHFORK BIFURCATION

Near a subcritical pitchfork bifurcation, the dynamics with noise along the slow manifold are described by the normal form [42]:

$$\dot{x} = 2\mu(t)x + 4x^3 + \epsilon\xi(t), \tag{20}$$

where μ is the bifurcation parameter, ϵ^2 is the noise strength, and ξ is zero-mean, delta-correlated white noise with autocorrelation $\langle\xi(t)\xi(t')\rangle = 2\delta(t-t')$. It is recognized that the presence of noise shifts the effective bifurcation parameter [46], so μ here includes that shift. The illustration of this system as a particle in an evolving potential is shown in Fig. 4. The FP equation corresponding with Eq. (20) is given by

$$\frac{\partial\rho}{\partial t} = -\frac{\partial}{\partial x}[(2\mu x + 4x^3)\rho] + \epsilon^2\frac{\partial^2\rho}{\partial x^2}, \tag{21}$$

where $\rho = \rho(x,t)$ is the probability distribution for the system state. As in the saddle-node case, we compare approximate results for fast and slow sweeping with numerical solutions of this FP equation.

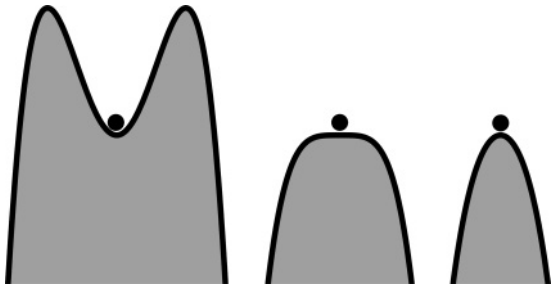

FIG. 4. Escape near a subcritical pitchfork bifurcation.

Suppose the system is initially near the local minimum $x = 0$ for $\mu < 0$. If μ is increased relatively slowly, $\epsilon^2 \gg \dot{\mu}$, the rate of escape can be approximated by the well-known adiabatic Kramers result [40,44], given by

$$W(t) = \frac{\sqrt{8}}{\pi}|\mu(t)|\exp\left[-\frac{\mu^2(t)}{4\epsilon^2}\right]. \tag{22}$$

The probability to remain in the well diminishes according to the product of this rate and the probability to remain in the well. Accordingly, the probability density function for escape at time T in the limit of adiabatic sweeping is given by [1,40]:

$$P(T) = W(T)\exp\left[-\int_{-t_0}^{T} W(t)dt\right]. \tag{23}$$

If μ is swept quickly, that is, $0 \leqslant \epsilon^2 \ll \dot{\mu}$, the system response is dominated by delayed bifurcations. However, the method employed for determining the distribution of escape events for the saddle-node bifurcation in this case is not convenient for the pitchfork, since here this approach does not yield a result independent of the initial conditions. This results from the fact that, for the pitchfork, the noise-free system maintains an equilibrium state, albeit unstable, beyond the bifurcation point. For the noise-free system, the initial conditions enter the solution multiplicatively and cannot be neglected. Nevertheless, diffusion removes the dependence on initial conditions when the parameter sweep is started sufficiently far from the bifurcation point, such that the system settles into a quasi-steady-state distribution [5,8,10]. To capture this effect we employ an alternative method for determining the distribution of escape times, using asymptotic expansions.

Following Suzuki [4], we separate the sweeping time into a first interval, over which nonlinear drift is ignored, and a second interval, over which diffusion is ignored. We show that, under some conditions stated below, there exists a time interval over which both approximations are valid, allowing one to match the solutions. A change of coordinates in Eq. (21) makes clear the two phases of response. Let

$$y = \frac{x}{\sigma}\text{where} \tag{24}$$

$$\sigma^2 = \epsilon^2 e^{4\int_{t_0}^{t}\mu\,dt'}\left(\sigma_0^2 + 2\int_{t_0}^{t} e^{-4\int_{t_0}^{t'}\mu\,dt''}dt'\right). \tag{25}$$

This particular σ^2 is the variance of the solution to the linearized problem in which the nonlinear drift term is neglected. By changing coordinates into one in which the linearized problem has a constant solution, we explicitly expose the role of nonlinear drift and its relationship to

diffusion. For simplicity, in this discussion we assume μ increases monotonically with t. In this case, the parameter σ has the following properties: it is positive, it takes on the value $\epsilon\sigma_0 \geqslant 0$ at time $t = t_0$, and it decreases until the time at which $2\mu\sigma^2/\epsilon^2 = -1$, which must occur before the bifurcation point is reached because μ must be negative to satisfy this condition. σ increases monotonically afterward. If the initial value is sufficiently small, $\sigma_0 < \epsilon/\sqrt{-2\mu_0}$, then σ increases monotonically. Taking y as the new coordinate, Eq. (21) becomes

$$\frac{\partial\rho}{\partial t} - \frac{\epsilon^2}{\sigma^2} y \frac{\partial\rho}{\partial y} = -2\mu\rho - 4\sigma^2 \frac{\partial}{\partial y}[y^3\rho] + \frac{\epsilon^2}{\sigma^2}\frac{\partial^2\rho}{\partial y^2}. \tag{26}$$

The second term on the left-hand side of Eq. (26) arises since y changes with time, t. The three terms on the right-hand side correspond to, in order, linear drift, nonlinear drift, and diffusion. In Eq. (26), the two regions of time become apparent by comparing the coefficients of the nonlinear drift and diffusion terms, namely, $4\sigma^2$ and ϵ^2/σ^2. The ratio of the two coefficients is

$$\frac{4\sigma^4}{\epsilon^2}. \tag{27}$$

In the initial phase of the response, this ratio is $\mathcal{O}(\epsilon^2)$ [assuming σ_0 is $\mathcal{O}(1)$], implying that diffusion dominates the nonlinear drift. At later times, the ratio is $\mathcal{O}(\epsilon^{-2})$, owing to the exponential growth of σ, and the nonlinear drift dominates diffusion. In the intermediate region, the ratio is $\mathcal{O}(1)$, and thus $\sigma^2 \sim \mathcal{O}(\epsilon)$. Delayed bifurcation dominates the system response when this overlap region occurs beyond the bifurcation point. Now, an upper bound for σ^2 at the bifurcation point, i.e., when $\mu = 0$, is $2\pi\epsilon^2/\min\dot{\mu}$, assuming μ is monotonically increasing. Thus, the condition $\epsilon^2 \ll \dot{\mu}$ ensures that the overlap region occurs after the bifurcation point and the system will exhibit delayed bifurcation.

In the initial time region we ignore the nonlinear drift with respect to diffusion and obtain an approximate solution ρ_l of Eq. (26) by solving

$$\frac{\partial\rho_l}{\partial t} = -2\mu\rho_l + \frac{\epsilon^2}{\sigma^2}\left(y\frac{\partial\rho_l}{\partial y} + \frac{\partial^2\rho_l}{\partial y^2}\right). \tag{28}$$

Taking a Gaussian initial condition with zero mean and variance σ_0^2, ρ_l is given by

$$\rho_l(y,t) = \frac{1}{\sqrt{2\pi\sigma^2}}\exp\left[-\frac{y^2}{2}\right]. \tag{29}$$

At the other end of the process, in the second time region, which leads to escape, diffusion can be ignored with respect to drift. An approximate solution $\rho_{\rm nl}$ of Eq. (26) for this case is obtained by solving

$$\frac{\partial\rho_{\rm nl}}{\partial t} = -2\mu\rho_{\rm nl} - 12\sigma^2y^2\rho_{\rm nl} - 4\sigma^2y^3\frac{\partial\rho_{\rm nl}}{\partial y}. \tag{30}$$

This equation is solved using the method of characteristics, which yields

$$\rho_{\rm nl}(y,t) = \rho_{\rm nl}^{(1)}(y_1,t_1)\left(\frac{y_1}{y}\right)^3\exp\left[-2\int_{t_1}^{t}\mu\,dt'\right], \tag{31}$$

$$y_1(y,t|t_1) = y\left[1 + y^2\int_{t_1}^{t}8\sigma^2\,dt'\right]^{-1/2}, \tag{32}$$

where $\rho_{\rm nl}^{(1)}(y_1,t_1)$ captures the constant of integration along each characteristic. This corresponds to the initial conditions for Eq. (30). Now, time t_1 need not be the starting time of the sweep, but can be taken to be any time before escape. To match the linear and nonlinear solutions, we take t_1 to be some time in the common region where the quantity in Eq. (27) is $\mathcal{O}(1)$. To do the matching, we choose $\rho_{\rm nl}^{(1)}$ such that $\rho_{\rm nl}$ and ρ_l are identical to the leading order in the common region.

We begin by rewriting Eq. (29) as

$$\rho_l = \frac{1}{\sqrt{2\pi}\sigma(t_1)}\exp\left[-\frac{y^2}{2} - 2\int_{t_1}^{t}\mu\,dt' - \int_{t_1}^{t}\frac{\epsilon^2}{\sigma^2}dt'\right]. \tag{33}$$

In the common region, the last integral is $\mathcal{O}(\epsilon)$, and it can be ignored, resulting in

$$\rho_l \approx \frac{1}{\sqrt{2\pi}\sigma(t_1)}\exp\left[-\frac{y^2}{2} - 2\int_{t_1}^{t}\mu\,dt'\right]. \tag{34}$$

Note that this is valid because t is not too far from t_1 as both are in the common region. By the same argument, we drop the integral in Eq. (32). Thus, $y_1 \approx y$ and the nonlinear solution is approximated by

$$\rho_{\rm nl} \approx \rho_{\rm nl}^{(1)}(y,t_1)\exp\left[-2\int_{t_1}^{t}\mu\,dt'\right]. \tag{35}$$

The two distributions are matched by taking

$$\rho_{\rm nl}^{(1)}(y_1,t_1) = \frac{1}{\sqrt{2\pi}\sigma(t_1)}\exp\left[-\frac{y_1^2}{2}\right]. \tag{36}$$

The probability to escape at time T can be understood as the probability current at $y = \infty$. In this limit, the linear drift and diffusion terms give zero since they cannot result in escape to ∞ in finite time. Thus, the escape current is computed from the nonlinear drift. Moreover, it is equally probable to escape to ∞ as to $-\infty$ owing to the symmetry of the problem. Accordingly, we can express the probability of escape at time T as twice the nonlinear probability current at $y = \infty$. The current is given by $P_\infty(T) = \lim_{y\to\infty} 8\sigma^2y^3\rho$. This gives

$$P_\infty = \frac{8\sigma^2(T)}{\sqrt{2\pi}}\left(8\int_{t_1}^{T}\sigma^2dt\right)^{-3/2} \times \exp\left[\int_{t_1}^{T}\frac{\epsilon^2}{\sigma^2}dt - \left(16\int_{t_1}^{T}\sigma^2dt\right)^{-1}\right]. \tag{37}$$

Equation (37) depends weakly on the choice of t_1, and, to leading order, this dependence can be removed, as follows. First, since ϵ^2/σ^2 is small for times after t_1, we drop the first integral in the exponent. Second, since σ^2 is small for times before t_1, we extend the lower bound of integration for the remaining integrals back to the bifurcation point, which is a well-defined time and makes a convenient choice. The resulting approximation is given by

$$P_\infty(T) \approx \frac{8\sigma^2(T)}{\sqrt{2\pi}}\left(8\int_{t_b}^{T}\sigma^2dt\right)^{-3/2} \times \exp\left[-\left(16\int_{t_b}^{T}\sigma^2dt\right)^{-1}\right], \tag{38}$$

where t_b is the time at which the noise-free bifurcation point is reached.

To solve a specific example, we again consider the linear sweep, for which $\mu = t$. In this case,

$$\sigma^2 = \epsilon^2 \sqrt{\frac{\pi}{2}} e^{2t^2} \left[\sqrt{\frac{2\sigma_0^4}{\pi}} e^{-2t_0^2} + \mathrm{erf}(\sqrt{2}t) - \mathrm{erf}(\sqrt{2}t_0) \right]. \tag{39}$$

For large $|t_0|$, that is, starting far from the bifurcation point, σ becomes approximately independent of σ_0 and t_0. Under this assumption, we take the approximation

$$\sigma^2 \approx \epsilon^2 \sqrt{\frac{\pi}{2}} e^{2t^2} (1 + \mathrm{erf}(\sqrt{2}t)). \tag{40}$$

For $\mu = t$, the bifurcation point is reached when $t = t_b = 0$. Thus, the integration of σ^2 gives

$$8 \int_0^T \sigma^2 dt = 2\pi\epsilon^2 \left[\mathrm{erfi}(\sqrt{2}\mathrm{T}) + \frac{4T^2}{\pi} {}_2F_2(2T^2) \right], \tag{41}$$

where erfi is the imaginary error function and ${}_2F_2$ is the hypergeometric function ${}_2F_2(1,1;3/2,2;2T^2)$ [45]. Thus, the escape distribution for a linear sweep is approximated by

$$P_\infty(T) \approx \frac{2[1 + \mathrm{erf}(\sqrt{2}T)]}{\sqrt{2\pi}\epsilon[\pi\,\mathrm{erfi}(\sqrt{2}T) + 4T^2 {}_2F_2(2T^2)]^{3/2}} \times \exp\left[-\frac{1}{4\epsilon^2[\pi\,\mathrm{erfi}(\sqrt{2}T) + 4T^2 {}_2F_2(2T^2)]} \right]. \tag{42}$$

Equation (42) is our primary result for the subcritical pitchfork bifurcation subject to the linear parameter sweep. Several aspects of this solution are illustrated in Fig. 5. The first three moments of the escape time are shown over a wide range of noise intensities, along with two sample distributions, computed using various numerical and approximate solutions of the FP equation. The mean (black) and variance (gray) are shown in panel (a), while the skewness is shown in panel (d). Panels (b) and (c) show sample escape distributions for large and small noise strengths (relative to the sweep rate), respectively, computed using the well-known adiabatic approximation (23) and Eq. (42), respectively. Solid lines indicate the solution obtained by numerically solving the FP equation over a finite domain. The moments for the adiabatic approximation (large noise) and the delayed bifurcation (small noise) approximation developed in this paper, Eq. (42), are shown as dashed lines. An interesting feature of the distributions is that the skewness is positive for delayed bifurcations and negative for activated escape, indicating that the sign of the skewness is an indicator of the noise strength relative to the sweep rate.

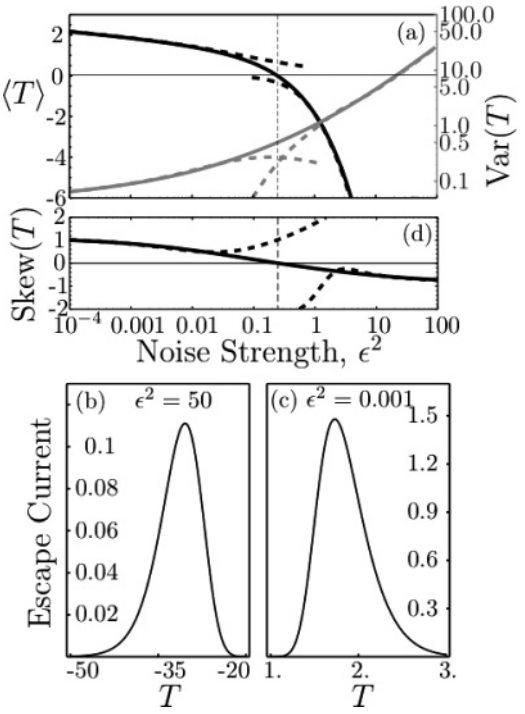

FIG. 5. Mean [(a), black], variance [(a), gray], and skew (d) of the escape current. Numeric solution (solid lines) and approximations (dashed lines) are shown. Two sample escape distributions are also shown, one for adiabatic escape (b) and one for delayed bifurcation (c).

IV. DISCUSSION AND CONCLUSIONS

In this paper, a systematic approach is taken to investigating the interplay between noise and parameter sweeps near bifurcations. Of particular interest are the saddle-node and subcritical pitchfork bifurcations, since these result in system responses that leave the vicinity of the bifurcating operating point, never to return, which we refer to as escape events. As described in the Introduction, these events are dramatic, easily detected, and relevant to a number of applications. By using the stochastic normal forms for these bifurcations, we determine the distribution of parameter values at which escape events occur during parameter sweeps. A general formulation is derived, based on the FP equation, which is solved numerically. The well-known adiabatic (Kramer) result is checked using an asymptotic approximation of the FP equation. The main contributions of the present investigation are approximate solutions derived for the case of small noise (relative to sweep rate), which result in delayed bifurcations. The results for both the saddle-node and subcritical pitchfork bifurcations are obtained using asymptotic expansion methods applied to the respective local normal form models, for which escape events are described by growth to infinity in finite time. These results are applicable to a wide class of systems for which the normal form describes behavior along the slow (center) manifold associated with the bifurcation. The predicted distributions for delayed bifurcations are valid over a range of parameters for which (i) the noise strength is much smaller than the bifurcation parameter sweep rate, $\epsilon^2 \ll |\dot{\mu}|$, and (ii) the normal form remains a valid model of the local dynamics, including the escape event. This places upper bounds on the system noise strength and sweep rates for which the results are valid. An additional feature of our results is that they provide a means of determining whether a given system will experience one of the limiting cases, namely, noise-activated escape or delayed bifurcation, or if it is in an intermediate range where one must deal more directly with the FP equation. These predictive results are quite generic, since they are based on normal

forms, and they have been successfully used for quantifying bifurcation detection in MEMS [29]. It is expected that they will be similarly useful for other systems that exhibit delayed bifurcations with large jumps in response amplitudes, such as nanomagnetic and Josephson-junction systems. Similar escape events will occur for subcritical Hopf bifurcations, but an investigation of this problem will require analysis of a two-dimensional normal form [47].

ACKNOWLEDGMENTS

The authors would like to extend a special acknowledgment to Professor Mark Dykman for fruitful discussion and insight. This material is based on work supported by the National Science Foundation under Grants No. CMMI-0758419 and No. CMMI-0900666 and by the Defense Advanced Research Project Agency under the MTO-DEFYS program.

[1] J. Kurkijärvi, Phys. Rev. B **6**, 832 (1972).
[2] L. D. Jackel, W. W. Webb, J. E. Lukens, and S. S. Pei, Phys. Rev. B **9**, 115 (1974).
[3] T. A. Fulton and L. N. Dunkleberger, Phys. Rev. B **9**, 4760 (1974).
[4] M. Suzuki, J. Stat. Phys. **16**, 477 (1977).
[5] G. Broggi, A. Colombo, L. A. Lugiato, and P. Mandel, Phys. Rev. A **33**, 3635 (1986).
[6] M. C. Torrent and M. SanMiguel, Phys. Rev. A **38**, 245 (1988).
[7] N. G. Stocks, R. Mannella, and P. V. E. McClintock, Phys. Rev. A **40**, 5361 (1989).
[8] H. Zeghlache, P. Mandel, and C. VandenBroeck, Phys. Rev. A **40**, 286 (1989).
[9] M. C. Torrent, F. Sagués, and M. SanMiguel, Phys. Rev. A **40**, 6662 (1989).
[10] N. G. Stocks, R. Mannella, and P. V. E. McClintock, Phys. Rev. A **42**, 3356 (1990).
[11] R. H. Victora, Phys. Rev. Lett. **63**, 457 (1989).
[12] W. Wernsdorfer, E.B. Orozco, K. Hasselbach, A. Benoit, B. Barbara, N. Demoncy, A. Loiseau, H. Pascard, and D. Mailly, Phys. Rev. Lett. **78**, 1791 (1997).
[13] K. M. Jansons and G. D. Lythe, J. Stat. Phys. **90**, 227 (1998).
[14] Y. Sang, M. Dubé, and M. Grant, Phys. Rev. Lett. **87**, 174301 (2001).
[15] M. H. Müser, M. Urbakh, and M. O. Robbins, in *Advances in Chemical Physics*, edited by I. Prigogine and S. A. Rice (Wiley, New York, 2003), Vol. 126, pp. 187–272.
[16] M. Urbakh, J. Klafter, D. Gourdon, and J. Israelachvili, Nature (London) **430**, 525 (2004).
[17] M. I. Dykman, Phys. Rev. E **81**, 051124 (2010).
[18] J. Atalaya, A. Isacsson, and M. I. Dykman, Phys. Rev. Lett. **106**, 227202 (2011).
[19] W. Tung, J. Hu, J. Gao, and V. Billock, Int. J. Bifurcation Chaos **18**, 1749 (2008).
[20] J. B. Gao, W. W. Tung, and N. Rao, Phys. Rev. Lett. **89**, 254101 (2002).
[21] S. K. Hwang, J. B. Gao, and J. M. Liu, Phys. Rev. E **61**, 5162 (2000).
[22] J. Gao, C. Chen, S. Hwang, and J. Liu, Int. J. Mod. Phys. B **13**, 3283 (1999).
[23] J. B. Gao, S. K. Hwang, and J. M. Liu, Phys. Rev. Lett. **82**, 1132 (1999).
[24] I. Siddiqi, R. Vijay, F. Pierre, C.M. Wilson, M. Metcalfe, C. Rigetti, L. Frunzio, and M.H. Devoret, Phys. Rev. Lett. **93**, 207002 (2004).
[25] I. Siddiqi *et al.*, *Quantum Computing in Solid State Systems* (Springer, New York, 2006), pp. 28–37.
[26] R. Vijay, M. H. Devoret, and I. Siddiqi, Rev. Sci. Instrum. **80**, 111101 (2009).
[27] F. Mallet *et al.*, Nature Physics **5**, 791 (2009).
[28] J. Thompson and J. Sieber, IMA J. Appl. Math. **76**, 27 (2011).
[29] C. B. Burgner, K. L. Turner, N. J. Miller, and S. W. Shaw, in Proceedings of the 13th Hilton Head Solid State Sensors and Actuators Conference, June 6–10, SC, USA, 2010 (unpublished).
[30] V. Kumar *et al.*, Appl. Phys. Lett. **98**, 153510 (2011).
[31] T. T. Heikkilä, P. Virtanen, G. Johansson, and F. K. Wilhelm, Phys. Rev. Lett. **93**, 247005 (2004).
[32] A. Lupascu *et al.*, Nature Physics **3**, 119 (2007).
[33] T. Novotný, J. Stat. Mech.: Theory Exp. (2009) P01050.
[34] D. F. Urban and H. Grabert, Phys. Rev. B **79**, 113102 (2009).
[35] Q. Le Masne, H. Pothier, N. O. Birge, C. Urbina, and D. Esteve, Phys. Rev. Lett. **102**, 067002 (2009).
[36] E. V. Sukhorukov and A. N. Jordan, Phys. Rev. Lett. **98**, 136803 (2007).
[37] I. Serban, M. I. Dykman, and F. K. Wilhelm, Phys. Rev. A **81**, 022305 (2010).
[38] N. Berglund and B. Gentz, *Noise-Induced Phenomena in Slow-Fast Dynamical Systems: A Sample-Paths Approach* (Springer, New York, 2006).
[39] M. Evstigneev, Phys. Rev. E **78**, 011118 (2008).
[40] P. Hanggi, J. Stat. Phys. **42**, 105 (1986).
[41] M. I. Dykman and M. A. Krivoglaz, Physica A **104**, 480 (1980).
[42] E. Knobloch and K. A. Wiesenfeld, J. Stat. Phys. **33**, 611 (1983).
[43] M. I. Dykman, B. Golding, and D. Ryvkine, Phys. Rev. Lett. **92**, 080602 (2004).
[44] H. A. Kramers, Physica **7**, 284 (1940).
[45] M. Abramowitz and I. A. Stegun, *Handbook of Mathematical Functions: with Formulas, Graphs, and Mathematical Tables* (Dover, New York, 1965).
[46] N. S. Namachchivaya, Applied Mathematics and Computation **38**, 101 (1990).
[47] L. Arnold, N. S. Namachchivaya, and K. R. Schenk-Hoppé, Int. J. Bifurcation Chaos **11**, 1947 (1996).